Journal of Biological Dynamics
Publication details, including instructions for authors and subscription information:
http://www.tandfonline.com/loi/tjbd20

Extracting the time-dependent transmission rate from infection data via solution of an inverse ODE problem

Mark Pollicott [a], Hao Wang [b] & Howard (Howie) Weiss [c]

[a] Mathematics Institute, University of Warwick, Coventry, CV4 7AL, UK

[b] Department of Mathematical and Statistical Sciences, University of Alberta, Edmonton, Alberta, Canada, T6G 2G1

[c] School of Mathematics, Georgia Institute of Technology, Atlanta, GA, 30332, USA

Version of record first published: 04 Jan 2012.

To cite this article: Mark Pollicott, Hao Wang & Howard (Howie) Weiss (2012): Extracting the time-dependent transmission rate from infection data via solution of an inverse ODE problem, Journal of Biological Dynamics, 6:2, 509-523

To link to this article: http://dx.doi.org/10.1080/17513758.2011.645510

Journal of Biological Dynamics
Vol. 6, No. 2, March 2012, 509–523

Taylor & Francis
Taylor & Francis Group

Extracting the time-dependent transmission rate from infection data via solution of an inverse ODE problem

Mark Pollicott[a], Hao Wang[b]* and Howard (Howie) Weiss[c]

[a]*Mathematics Institute, University of Warwick, Coventry, CV4 7AL, UK;* [b]*Department of Mathematical and Statistical Sciences, University of Alberta, Edmonton, Alberta, Canada T6G 2G1;* [c]*School of Mathematics, Georgia Institute of Technology, Atlanta, GA 30332, USA*

(*Received 15 June 2011; final version received 26 November 2011*)

The transmission rate of many acute infectious diseases varies significantly in time, but the underlying mechanisms are usually uncertain. They may include seasonal changes in the environment, contact rate, immune system response, etc. The transmission rate has been thought difficult to measure directly. We present a new algorithm to compute the time-dependent transmission rate directly from prevalence data, which makes no assumptions about the number of susceptible or vital rates. The algorithm follows our complete and explicit solution of a mathematical inverse problem for SIR-type transmission models. We prove that almost any infection profile can be perfectly fitted by an SIR model with variable transmission rate. This clearly shows a serious danger of overfitting such transmission models. We illustrate the algorithm with historic UK measles data and our observations support the common belief that measles transmission was predominantly driven by school contacts.

Keywords: epidemiology; time-dependent transmission rate; extraction algorithm; inverse problem; measles; modulus of Fourier transform, Fourier analysis; periodicity; overfitting

1. Introduction

The transmission rate of an infectious disease is the *per capita* rate of infection given contact. It is the epidemiological analogue of a rate constant in chemical reactions. In Section 3.4.9 of Anderson and May [1], the authors state that '. . . the direct measurement of the transmission rate is essentially impossible for most infections. But if we wish to predict the changes wrought by public health programmes, we need to know the transmission rate . . .' . The transmission rate of many acute infectious diseases varies significantly in time and frequently exhibits significant seasonal dependence [3,6,9,16,28,33]: influenza, pneumococcus, and rotavirus cases peak in winter; respiratory syncytial virus and measles cases peak in spring; and polio cases peak in summer.

Most investigators *define* the transmission rate $\beta(t)$ of an infectious disease via the discrete transmission model:

$$S(k+1) = S(k) - I(k+1), \tag{1}$$

*Corresponding author. Email: hwang@math.ualberta.ca, hao8@ualberta.ca
Author Emails: mpollic@maths.warwick.ac.uk; weiss@math.gatech.edu

ISSN 1751-3758 print/ISSN 1751-3766 online

http://dx.doi.org/10.1080/17513758.2011.645510
http://www.tandfonline.com

$$I(k+1) = \beta(k)S(k)I(k), \tag{2}$$

where $S(k), I(k)$ are the fractions of susceptible and infected individuals during week k [2,11]. Equation (2) is equivalent to $\beta(k) = I(k+1)/[I(k)S(k)]$, which provides a formula for the transmission rate. The application of this 'algorithm' requires knowledge of $S(0)$, which is sometimes difficult to estimate, especially for outbreaks where a sizable proportion of the population is immune to infection. An example is the elderly population during the 2009 H1N1 pandemic. We developed our algorithm, in part, to avoid having to estimate $S(0)$. See [14] for other issues with using Equations (1) and (2), as well as various extensions and simplifications of our algorithm.

Our new algorithm is based on the solution of a mathematical inverse problem for SIR-type transmission models using ordinary differential equations. We first consider the simplest SIR model [22] and allow the transmission rate to be a time-dependent function, i.e. there is a positive function $\beta(t)$ such that

$$S'(t) = -\beta(t)S(t)I(t), \tag{3}$$

$$I'(t) = \beta(t)S(t)I(t) - \nu I(t), \tag{4}$$

$$R'(t) = \nu I(t), \tag{5}$$

where $S(t), I(t)$, and $R(t)$ are the fractions of susceptible, infected, and removed individuals at time t. We pose the mathematical question:

Given 'smooth prevalence data' $f(t)$ on time interval $[0, T]$ and removal rate $\nu > 0$, can one always find a non-negative transmission rate function $\beta(t)$ such that the $I(t)$ output of the SIR model always coincides with $f(t)$ with the given ν?

Mathematicians call this an inverse problem. We prove that this is always possible subject to a mild restriction on the data and ν, and we provide an explicit formula for the solution. The construction also illustrates the danger of overfitting a transmission model where one can choose the time-dependent transmission rate.

However, in practice, prevalence data are always discrete, not continuous. We show that one can compute $\beta(t)$ by first smoothly interpolating the data with a spline or trigonometric function and then applying the formula to smooth data. The output of the SIR model with this $\beta(t)$ will coincide exactly with the data.

The usual transmission rate estimation method based on (1) and (2) can be viewed as a discretization of (3) and (4). However, unlike the discrete extraction method, our approach yields an explicit formula for the transmission rate, and also extends to a large spectrum of transmission models (see Section 4.1).

One of the extensions in Section 4.1 is to the SEIR epidemic model with historical (time-dependent) vital rates, and we illustrate this extended algorithm using monthly UK measles notification data during 1948–1966. Our extracted transmission rate exhibits two dominant spectral peaks: at frequencies 1 and 3 per year, respectively. We show that the latter peak reflects the 'cycle' of Christmas, Easter, and Summer school vacations. These observations support the common belief that measles transmission is predominantly driven by school contacts [13,21]. However, we also find indications of a cycle with a 2-year period. Although our method requires prevalence data, for measles the notification data suffices to generate correct dominant frequencies of $\beta(t)$.

2. Results

We first derive the algorithm for extracting the time-dependent transmission rate from prevalence data. We then apply the algorithm to two simulated data sets representing two characteristic 'types' of infectious diseases. Finally, we illustrate the algorithm, using UK measles data from 1948 to 1966.

2.1. *Solution of inverse problem*

The new algorithm follows from the complete solution of an inverse problem for the SIR system of ODEs. The generality of the result seems striking, while the proof is almost trivial.

THEOREM 2.1 *Given a smooth positive function $f(t)$, $\nu > 0$, $\beta_0 > 0$, and $T > 0$, there exists $K > 0$ such that if $\beta_0 < K$ there is a solution $\beta(t)$ with $\beta(0) = \beta_0$ such that $I(t) = f(t)$ for $0 \le t \le T$ if and only if $f'(t)/f(t) > -\nu$ for $0 \le t \le T$.*

The growth condition imposes no restrictions on how $f(t)$ increases, but requires that $f(t)$ cannot decrease too quickly, in the sense that its logarithmic derivative is always bounded below by $-\nu$. It is easy to see that $f'(t)/f(t) > -\nu$ is a necessary condition, since Equation (4) implies that $f'(t) + \nu f(t) = \beta(t)S(t)f(t)$, which must be positive for $0 \le t \le T$.

The proof of the theorem consists of showing that this condition is also sufficient. We rewrite Equation (4) as

$$S(t) = \frac{f'(t) + \nu f(t)}{\beta(t) f(t)}, \tag{6}$$

then compute $S'(t)$, and then equate with Equation (3) to obtain

$$\frac{\mathrm{d}}{\mathrm{d}t}\left(\frac{f'(t) + \nu f(t)}{\beta(t) f(t)}\right) = -\beta(t)\left(\frac{f'(t) + \nu f(t)}{\beta(t) f(t)}\right) f(t). \tag{7}$$

Calculating the derivative and simplifying the resulting expression yields the following Bernoulli differential equation for $\beta(t)$

$$\beta'(t) - p(t)\beta(t) - f(t)\beta^2(t) = 0, \quad \text{where } p(t) = \frac{f''(t)f(t) - f'(t)^2}{f(t)(f'(t) + \nu f(t))}. \tag{8}$$

The change of coordinates $x(t) = 1/\beta(t)$ transforms this nonlinear ODE into the linear ODE

$$x'(t) + p(t)x(t) + f(t) = 0. \tag{9}$$

The method of integrating factors provides the explicit solution

$$\frac{1}{\beta(t)} = x(t) = x(0)\mathrm{e}^{-P(t)} - \mathrm{e}^{-P(t)} \int_0^t \mathrm{e}^{P(s)} f(s)\,\mathrm{d}s, \quad \text{where } P(t) = \int_0^t p(\tau)\,\mathrm{d}\tau. \tag{10}$$

A problem that could arise with this procedure is for the denominator of $p(t)$ to be zero. A singular solution is prevented by requiring that the denominator be always positive, i.e. $f'(t) + \nu f(t) > 0$. Having done this, to ensure that $\beta(t)$ is positive, $\beta(0)$ must satisfy

$$\int_0^{\mathrm{T}} \mathrm{e}^{P(s)} f(s)\,\mathrm{d}s < \frac{1}{\beta(0)}. \tag{11}$$

Mathematically, there are infinitely many choices of $\beta(0)$ and thus infinitely many transmission functions $\beta(t)$. In this sense, the inverse problem is under-determined.

2.2. *Extraction algorithm*

We now turn the proof of the theorem into an algorithm to extract the transmission rate $\beta(t)$ from a prevalence data set. The algorithm has four steps and requires two conditions.

Step 1. Smoothly interpolate the infection data with a spline or trigonometric function to generate a smooth $f(t)$. Check condition 1: $f'(t)/f(t) > -\nu$, where ν is the removal rate.

Step 2. Compute the function $p(t) = (f''(t)f(t) - f'(t)^2)/(f(t)(f'(t) + \nu f(t)))$. Condition 1 prevents a zero denominator in $p(t)$.

Step 3. Choose $\beta(0)$ and compute the integral $P(t) = \int_0^t p(\tau)\,\mathrm{d}\tau$. Check condition 2: $\beta(0) < 1/\int_0^T \mathrm{e}^{P(s)} f(s)\,\mathrm{d}s$, where T is the time length of the infection data. Alternatively, choose $\beta(0)$ sufficiently small to satisfy condition 2.

Step 4. Apply the formula $\beta(t) = 1/[\mathrm{e}^{-P(t)}/\beta(0) - \mathrm{e}^{-P(t)} \int_0^t \mathrm{e}^{P(s)} f(s)\,\mathrm{d}s]$ to compute $\beta(t)$ on the given interval $[0, T]$.

Condition 1 is equivalent to $\mathrm{d}(\ln f(t))/\mathrm{d}t > -\nu$, i.e. the time series of infection data cannot decay too fast at any time. The expression $\mathrm{d}(\ln f(t))/\mathrm{d}t = f'(t)/f(t) = \beta(t)S(t) - \nu = \nu(R_e(t) - 1)$, where $R_e(t)$ is the effective reproduction rate at time t. The violation of Condition 1 would result in $R_e(t_0) \leq 0$ for some $t_0 > 0$. This is a mild condition that most data sets should satisfy. If a data set does not satisfy this condition, we propose a scaling trick in Section 3 to be able to apply the algorithm.

In Section 4.1, we present extensions of the basic extraction algorithm to several popular extensions of the SIR model, including the SEIR model with variable vital rates. Our algorithm can be extended to virtually any such compartment model.

2.3. *Extracting the transmission rate from simulated data*

We first illustrate the extraction algorithm using two simulated data sets. The functions $f(t)$ and $g(t)$ are the fractions of the infected population for two characteristic 'types' of infectious diseases.

The first data set simulates an infectious disease with periodic outbreaks, as observed in measles (before mass vaccination) and cholera [24,29]. The periodic function $f(t) = 10^{-5}[1.4 + \cos(1.5t)]$ represents the continuous infection data, and Figure 1(a) contains plots of both $f(t)$ (solid) and its associated transmission rate function $\beta(t)$ (dashed).

The second data set simulates an infectious disease with periodic outbreaks that decays in time, as observed in influenza [31]. The periodic function $g(t) = 10^{-5}[1.1 + \sin(t)]\exp(-0.1t)$ represents the continuous infection data, and Figure 2(a) contains plots of both $g(t)$ (solid) and its associated transmission rate function $\beta(t)$ (dashed).

We extract discrete data from functions $f(t)$ and $g(t)$ by sampling them at equi-spaced intervals (see the small black squares in Figures 1(a) and 2(a)). To each discrete time series, we apply two well-known interpolation algorithms (trigonometric approximation and spline approximation) [23,32]. Figures 1(b) and 2(b) contain plots of $\beta(t)$ obtained from the two smooth interpolations together with the extraction algorithm. Both interpolation schemes yield excellent approximations of $\beta(t)$ in both examples.

Many simulations show that the extraction algorithm is robust, maintaining the pattern of $\beta(t)$, with respect to white noise up to 10% of the data mean, as well as varying the number of sample points.

2.4. *Extracting the transmission rate from UK measles incidence data*

Previous studies [10,20] employed the SEIR model with vital rates to explore the epidemic and endemic behaviours of measles infections, using the notification data in [30]. To compare our new extraction technique with previous measles studies, we extend our extraction algorithm to the SEIR model with variable vital rates (see Section 4.1.5) and use the same data set. To examine the robustness of our new results, we post-condition the data to account for underreporting and reapply the extended extraction algorithm.

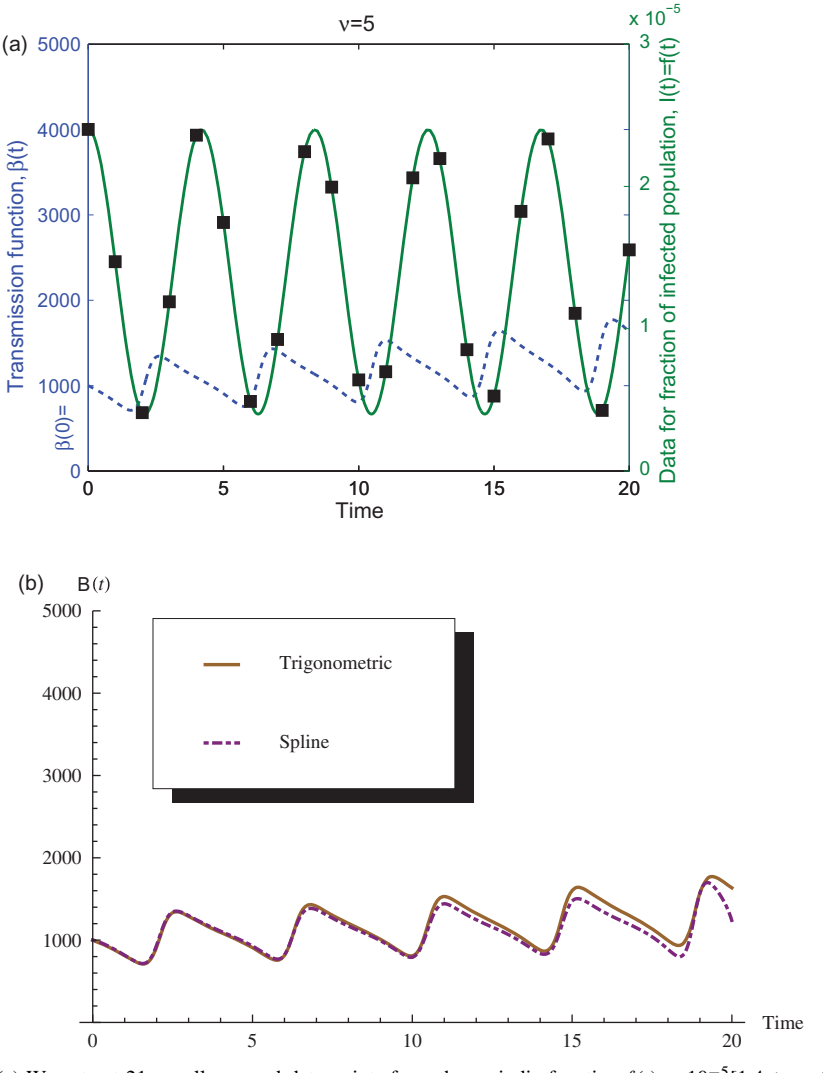

Figure 1. (a) We extract 21 equally spaced data points from the periodic function $f(t) = 10^{-5}[1.4 + \cos(1.5t)]$; the dashed curve is $\beta(t)$ extracted from $f(t)$, using Equation (10). (b) These transmission functions are estimated, using spline and trigonometric interpolations on the 21 data points.

We use the measles parameter values from Anderson and May [1,30]: $\nu = 52/\text{year} = 52/12/\text{month}$ (where $1/\nu$ is the removal period), $a = 52/\text{year} = 52/12/\text{month}$ (where $1/a$ is the latent period), and $\delta = 1/70/\text{year} = 1/70/12/\text{month}$ (death rate, equivalent to the life span of 70 years).

Public databases, such as the International Infectious Disease Data Archive [18] and Bolker's measles data archive [17], contain the weekly numbers of measles notifications from 1948 to 1966 and the quarterly reported historical UK births from 1948 to 1956. During 1948–1956 the births show large annual variations (see Figure 3(c)) with a strong 1/year frequency component (see Figure 3(d)). Since some years, these variations approach 20%, we include actual births in our model. Since neither database contains the UK birth rates from 1957 to 1966, this requires us to restrict our study to the period 1948–1956.

Previous measles modellers have used notification data (the number of reported new infections during a given period) as a surrogate for prevalence data (the total number of infections during

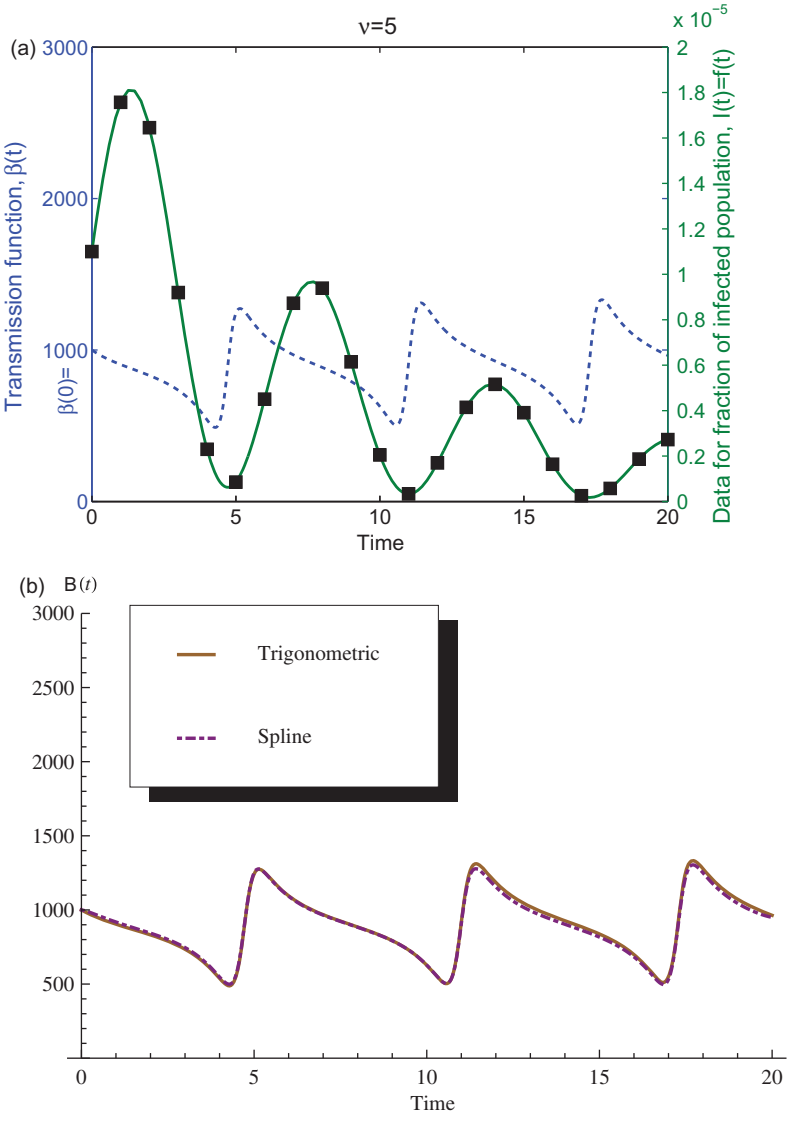

Figure 2. (a) We extract 21 equally spaced data points from the oscillatory decaying function $g(t) = 10^{-5}[1.1 + \sin(t)]\exp(-0.1t)$; the dashed curve is $\beta(t)$ extracted from $g(t)$, using Equation (10). (b) These transmission functions are estimated, using spline and trigonometric interpolations on the 21 data points.

the period) [10,35]. To be able to compare our results with those of previous authors, we first apply our extraction algorithm to the same notification data. We then apply the standard method to convert the notification data to prevalence data and apply our algorithm to the estimated prevalence data. The resulting $\beta(t)$ from these two data sets have same dominant frequencies (see Figures 4 and 5). Hence, for measles the notification data suffices to generate correct dominant frequencies of $\beta(t)$.

Since the birth data are provided only quarterly and the notifications weekly, we smoothly interpolate the birth data and aggregate the notification data into one month intervals. To aggregate weekly infection data into monthly data, we simply sum the weekly data as previous studies [10,35]. For a week across 2 months, this weekly infection number is separated to be two parts. For instance, if 1 week has 3 days in May and 4 days in June, then we multiply the number of

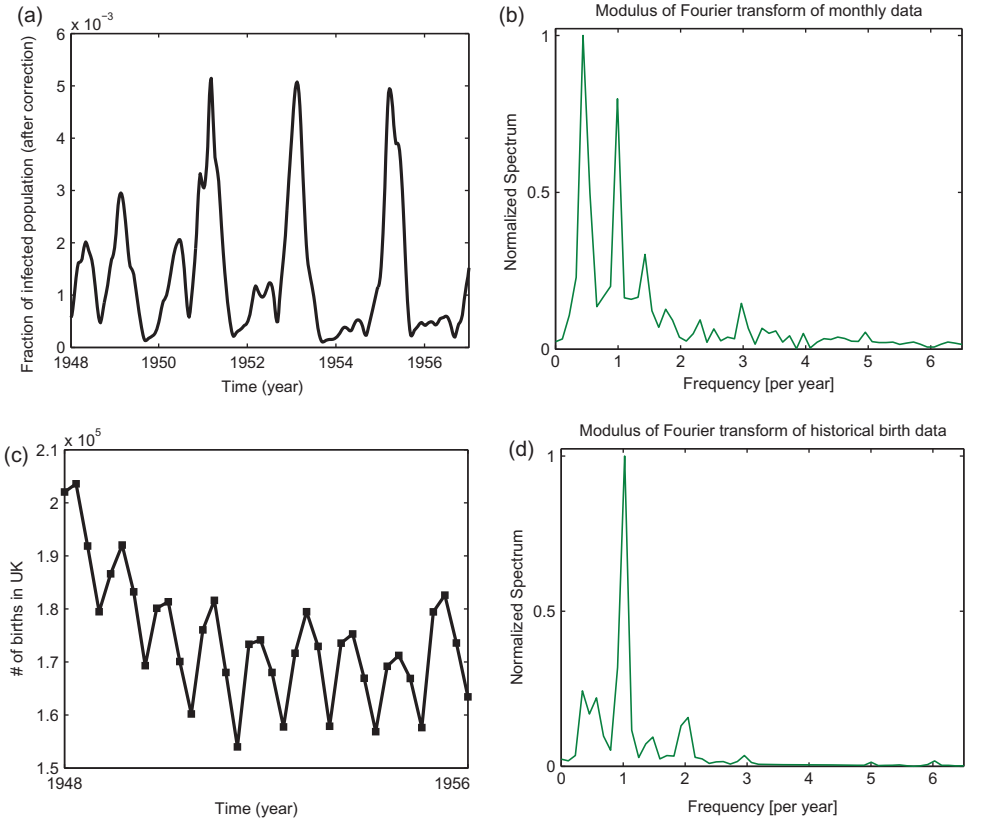

Figure 3. (a) Aggregated monthly measles data from England and Wales in 1948–1956. (b) Fourier transform of filtered and smoothly interpolated aggregated monthly data showing the dominant frequency components (normalized modulus). Note: We filter and remove the artificial peak at zero frequency in the Fourier transform. (c) UK birth rates during 1948–1956. (d) Fourier transform of smoothly interpolated UK birth data showing the dominant frequency component (normalized modulus).

notifications during this week by 3/7 and incorporate it into the May data, and we multiply the number of notifications during this week by 4/7 and incorporate it into the June data.

In Figure 4(a), (c) ,(e), and (g), we plot the transmission rates $\beta(t)$ extracted from our algorithm for four different January initial values chosen to represent a wide range of $\beta(0)$. The graphs of the extracted $\beta(t)$ in panels (e) and (g) are stationary, exhibit a slowly increasing drift in panel (c), and exhibit a faster increasing drift in panel (a). Note that in all cases, the annual minima occur in July–August during the summer school vacation period and that the annual maxima occur in January or September during the first month after the winter and summer school vacations.

In Figure 4(b), (d), (f), and (h), we plot the moduli of the Fourier transform of all extracted $\beta(t)$ and observe that there are two competing dominant spectral peaks. These two dominant peaks have 1 and 1/3-year periods. The three per year (i.e. 1/3-year period) peak of $\beta(t)$ seems to be due to the three major school terms, which are separated by the Christmas, Easter, and Summer breaks (see Figure 6). For stationary $\beta(t)$ (see panels (e), (g)), the one per year spectral peak is dominant (see panels (f), (h)), and the one half per year (2-year period) spectral peak is comparable to the three per year spectral peak (see panel (h)). We conclude that for a huge range of $\beta(0)$, the transmission rate always possesses both strong 1 and 1/3-year cycles.

To test the robustness of our spectral peaks, we incorporate the standard correction factor of 92.3% to account for the underreporting bias in the UK measles data (with estimated mean

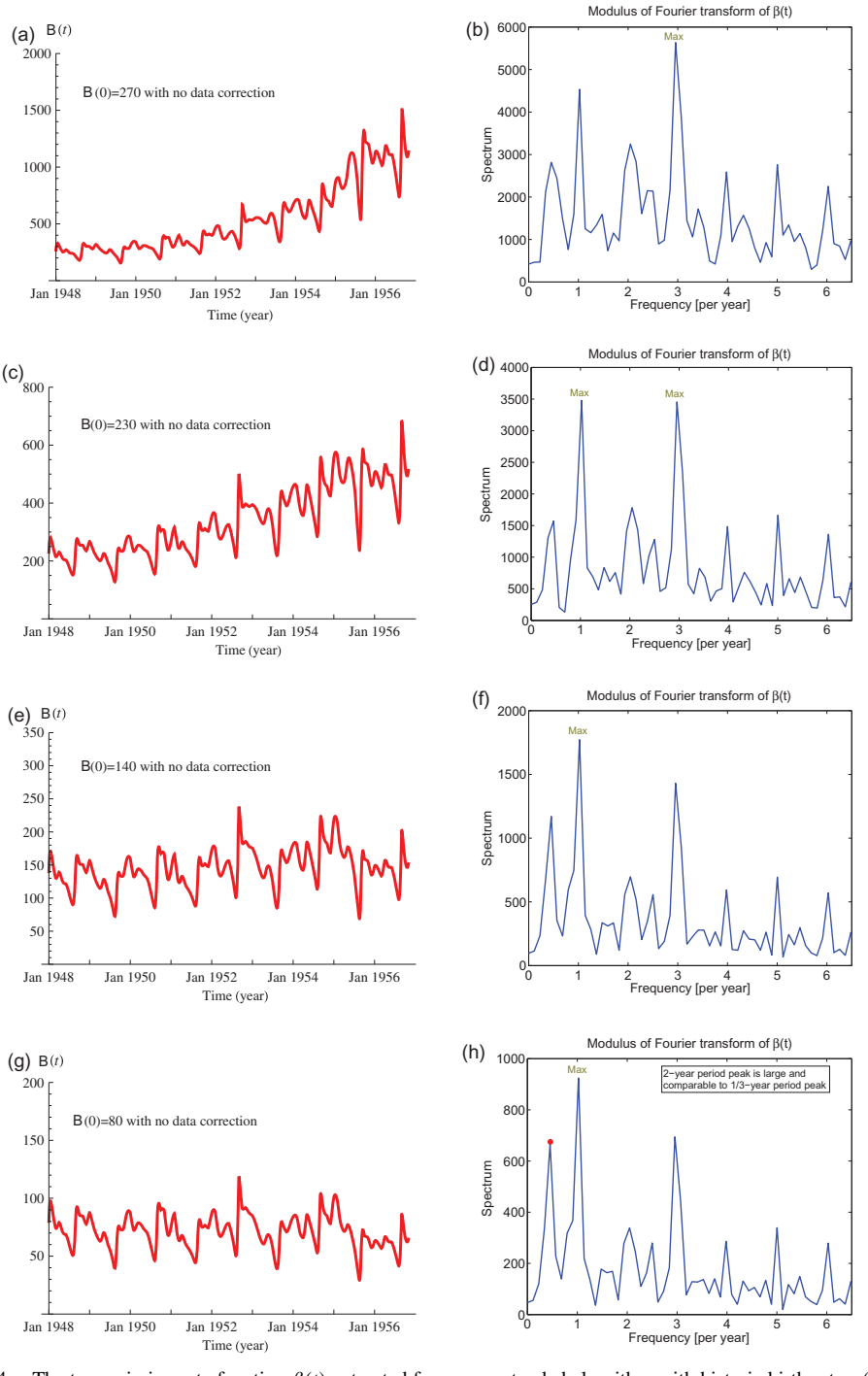

Figure 4. The transmission rate function $\beta(t)$ extracted from our extended algorithm with historic birth rates. (a) The extracted $\beta(t)$ with $\beta(0) = 270$: fast increasing peaks. (b) Fourier transform of filtered $\beta(t)$ showing the dominant frequency component, 3 per year. (c) The extracted $\beta(t)$ with $\beta(0) = 230$: slowly increasing peaks. (d) Fourier transform of filtered $\beta(t)$ showing two comparable dominant frequencies components, 1 and 3 per year. (e) The extracted $\beta(t)$ with $\beta(0) = 140$: stationary peaks. (f) Fourier transform of filtered $\beta(t)$ showing the dominant frequency component, 1 per year. (g) The extracted $\beta(t)$ with $\beta(0) = 80$: stationary peaks. (h) Fourier transform of filtered $\beta(t)$ showing the dominant frequency component, 1 per year; $1/2$ per year peak is large and comparable to the 3 per year peak.

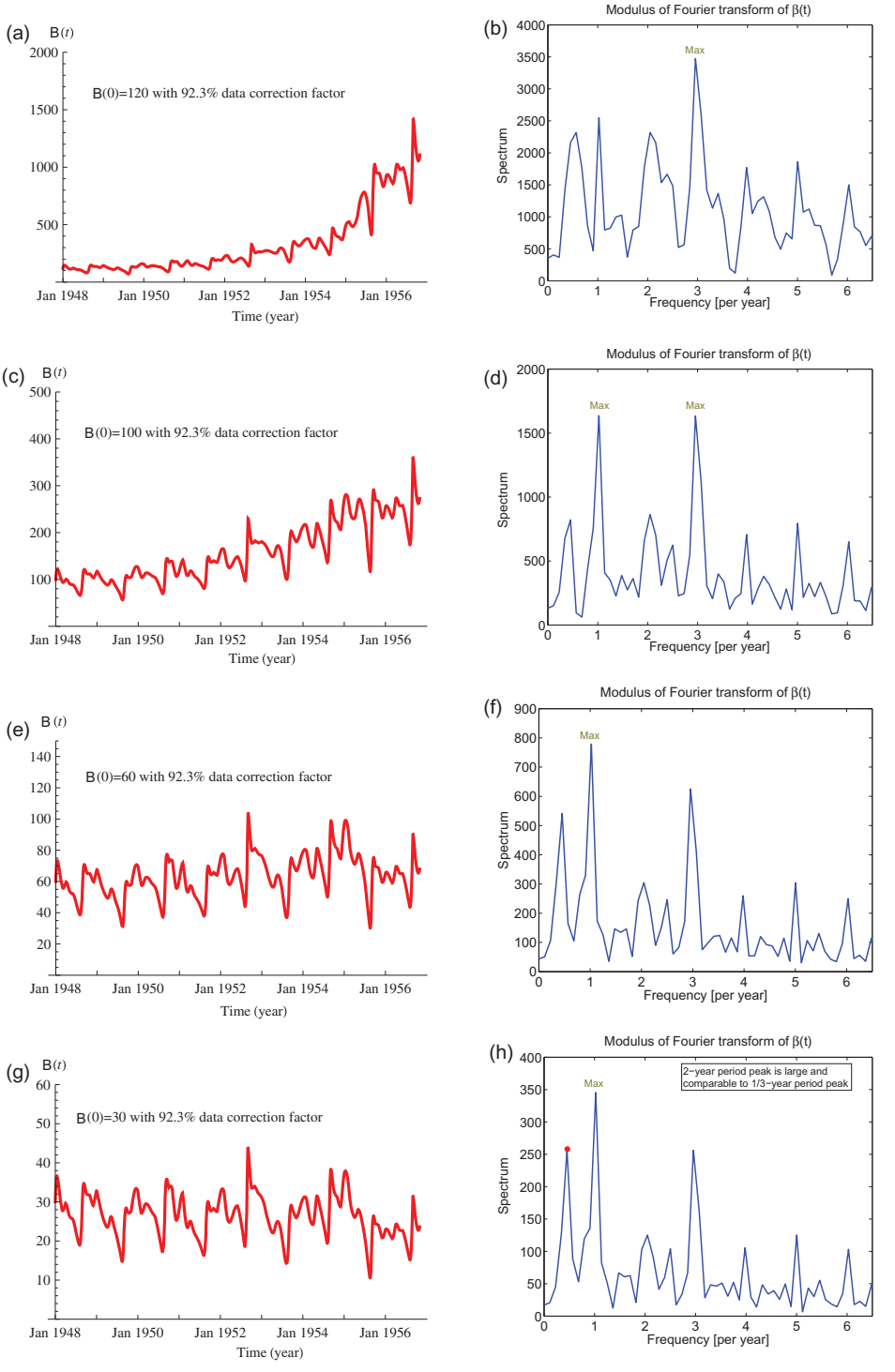

Figure 5. We test our estimations of $\beta(t)$ with data correction. The moduli of Fourier transform of $\beta(t)$ with the 92.3% correction factor have identical spectral peaks as those without data correction in Figure 4. (a) The extracted $\beta(t)$ with $\beta(0) = 120$. (c) The extracted $\beta(t)$ with $\beta(0) = 100$. (e) The extracted $\beta(t)$ with $\beta(0) = 60$. (g) The extracted $\beta(t)$ with $\beta(0) = 30$. Panels (b), (d), (f), and (h) plot moduli of Fourier transform of corresponding $\beta(t)$ in (a), (c), (e), and (g), respectively.

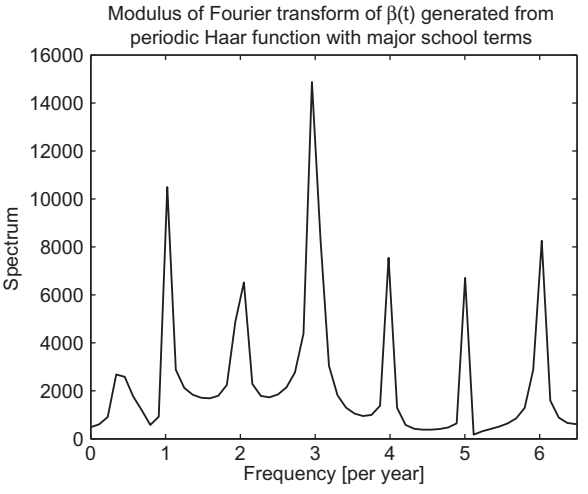

Figure 6. The transmission rate $\beta(t)$ is generated from the Haar function with major school holidays via aggregation. The modulus of Fourier transform of $\beta(t)$ generated from the widely used periodic Haar function shows the dominant three times per year frequency.

reporting rate 52%, note that 92.3% is computed from $1/0.52 - 1$) [4,8,34]. Since both the removal stage in the SEIR model and the infection notification period are 1 week, and the 92.3% correction factor essentially doubles the number of cases, this corrected number of cases will account for the non-notified cases during the removal stage. Hence, the corrected weekly notification data should provide a good approximation for total weekly infections. This precise methodology was used in [4,5].

In Figure 5, we plot the extracted $\beta(t)$ with the 92.3% correction factor and for the large range of $\beta(0)$. All the extracted $\beta(t)$ have identical dominant frequencies as those in Figure 4. Thus our observation of the two spectral peaks with frequencies 1/year and 3/year seems strongly robust. Again, we observe that the scale of the infection data regulates the scale of $\beta(t)$, but does not affect dominant frequencies of $\beta(t)$.

Most previous measles models represent the time-varying transmission rate, using a school term-time forcing function (such as the sinusoidal or the Haar function), and fitted parameters using the method of least squares. None seem to provide variances for their estimates [5]. Little empirical evidence currently supports their assumed functions that ignore other seasonal factors such as environmental changes and immune system changes [12,27]. However, our observations support this common belief that measles transmission is predominantly driven by school contacts.

3. Discussion

We present a new algorithm to compute the time-dependent transmission rate from prevalence data, which makes no assumptions about the number of susceptible or vital rates. We do have to estimate $\beta(0)$, which can be a formidable challenge. By manipulating our derivation, Hadeler recently derived another inversion formula for $\beta(t)$ that requires knowledge of $S(0)$ instead of $\beta(0)$ [14]. Hadeler's paper [14] also includes a formula that can be applied to notification data, however, our formula is only applicable to prevalence data.

Our algorithm can be viewed as a continuous version of the well-known discrete method for estimating the time-varying transmission rate. The inverse method in this paper can be applied to derive the extraction algorithms for a large spectrum of epidemiological models (see Section 4.1).

In this sense, our new method provides a more general method than the discrete method since it can account for factors such as the transmission mode and the immunity memory period, which can have a significant effect on transmission rate.

We illustrate the extraction algorithm for the SEIR model with variable vital rates, using UK measles data from 1948 to 1956. The Fourier transform of our extracted transmission rate function shows dominant spectral peaks at frequencies 1 and 3 per year. The 3 per year frequency seems to arise from the three major school breaks. Our observations support the common belief that measles transmission is predominantly driven by school contacts, but we also find indications of a 2-year cycle.

Our algorithm has some limitations to its applicability. First, the proportion of infected individuals, $f(t)$, cannot decrease too fast over the full time interval of interest. In general, one can add a sufficiently large constant to $f(t)$ to ensure this, but this will change the range of applicable $\beta(0)$, and applicability needs to be checked case by case. Second, one must assume that the proportion (or number) of notifications is always strictly positive. In practice, this restriction can be overcome by replacing zero values in the time series with a very small positive value. Third, for a chosen $\beta(0)$, the algorithm may only apply to a finite length of infection data. Finally, one either needs to know the value of the transmission rate at some fixed time, or verify that the claimed properties of $\beta(t)$ hold for all $\beta(0)$ attaining a large range of values.

We believe that the algorithm should apply to the vast majority of infection data sets (Mummert [25], Mummert *et al.* [26] apply the algorithm or an extended version to influenza data), and as a consequence, one can nearly always construct a time-dependent transmission rate $\beta(t)$ such that the SIR model will perfectly fit data. This illustrates a potential danger of overfitting an epidemic model with time-dependent transmission rate.

Recently, likelihood-based methods for estimating the time-varying transmission function have been developed in [7,15], using stochastic transmission models. Our algorithm can also be extended to incorporate stochastic effects by using stochastic differential equations.

4. Materials and methods

4.1. *Extensions of the basic model*

Analogous results and inversion formulae hold for all standard variations of the standard SIR model and their combinations. The proofs are similar to the proof of Theorem 2.1. Here, we only present the full algorithm for the SEIR model with vital rates, since we apply this algorithm to UK measles data.

4.1.1. *SIR model with vital rates*

$$S'(t) = \delta - \beta(t)S(t)I(t) - \delta S(t), \tag{12}$$

$$I'(t) = \beta(t)S(t)I(t) - \nu I(t) - \delta I(t), \tag{13}$$

$$R'(t) = \nu I(t) - \delta R(t). \tag{14}$$

The necessary and sufficient condition for extracting $\beta(t)$ given ν and δ is $f'(t)/f(t) > -(\nu + \delta)$.

4.1.2. *SIR model with waning immunity*

$$S'(t) = mR(t) - \beta(t)S(t)I(t), \tag{15}$$

$$I'(t) = \beta(t)S(t)I(t) - \nu I(t), \tag{16}$$

$$R'(t) = \nu I(t) - mR(t), \tag{17}$$

where $1/m$ is the memory period of immunity. The necessary and sufficient condition for extracting $\beta(t)$ given ν is $f'(t)/f(t) > -\nu$.

4.1.3. *SIR model with time-dependent indirect transmission rate* [19]

$$S'(t) = -\omega(t)S(t), \tag{18}$$

$$I'(t) = \omega(t)S(t) - \nu I(t), \tag{19}$$

$$R'(t) = \nu I(t), \tag{20}$$

where $\omega(t)$ is the time-dependent indirect transmission rate. The necessary and sufficient condition for extracting $\beta(t)$ given ν is $f'(t)/f(t) > -\nu$.

4.1.4. *SEIR model*

$$S'(t) = -\beta(t)S(t)I(t), \tag{21}$$

$$E'(t) = \beta(t)S(t)I(t) - \alpha E(t), \tag{22}$$

$$I'(t) = \alpha E(t) - \nu I(t), \tag{23}$$

$$R'(t) = \nu I(t), \tag{24}$$

where $1/\alpha$ is the latent period for the disease. By simple calculations, we can show that the necessary and sufficient condition for extracting $\beta(t)$ from infection data is $f'(t)/f(t) > -\nu$.

4.1.5. *SEIR model with vital rates*

$$S'(t) = \delta - \beta(t)S(t)I(t) - \delta S(t), \tag{25}$$

$$E'(t) = \beta(t)S(t)I(t) - aE(t) - \delta E(t), \tag{26}$$

$$I'(t) = aE(t) - \nu I(t) - \delta I(t), \tag{27}$$

$$R'(t) = \nu I(t) - \delta R(t). \tag{28}$$

The necessary and sufficient conditions for extracting $\beta(t)$ from infection data are

$$f'(t) + (\nu + \delta)f(t) > 0 \quad \text{and} \quad f''(t) + (\nu + 2\delta + a)f'(t) + (\delta + a)(\nu + \delta)f(t) > 0. \tag{29}$$

In this case, $\beta(t)$ satisfies the Bernoulli equation

$$\beta' + p(t)\beta + q(t)\beta^2 = 0, \tag{30}$$

where

$$p(t) = \frac{\begin{array}{c}-af'''(t)f(t) - a(\nu+2\delta+a)f''(t)f(t) - a(\delta+a)(\nu+\delta)f'(t)f(t) + af''(t)f'(t)\\ +a(\nu+2\delta+a)f'(t)^2\end{array}}{af(t)[f''(t)+(\nu+2\delta+a)f'(t)+(\delta+a)(\nu+\delta)f(t)]}$$
$$+\frac{\begin{array}{c}a(\delta+a)(\nu+\delta)f'(t)f(t) - \delta af''(t)f(t) - \delta a(\nu+2\delta+a)f'(t)f(t)\\ -\delta a(\delta+a)(\nu+\delta)f^2(t)\end{array}}{af(t)[f''(t)+(\nu+2\delta+a)f'(t)+(\delta+a)(\nu+\delta)f(t)]},$$

and

$$q(t) = \frac{\delta a^2 f^2(t) - af''(t)f^2(t) - a(\nu+2\delta+a)f'(t)f^2(t) - a(\delta+a)(\nu+\delta)f^3(t)}{af(t)[f''(t)+(\nu+2\delta+a)f'(t)+(\delta+a)(\nu+\delta)f(t)]}.$$

The modified extraction algorithm has five steps together with three conditions.

Step 1. Smoothly interpolate the infection data to generate a smooth function $f(t)$ that has at least a continuous second derivative. Check condition 1: $f'(t)+(\nu+\delta)f(t) > 0$; and check condition 2: $f''(t)+(\nu+2\delta+a)f'(t)+(\delta+a)(\nu+\delta)f(t) > 0$.

Step 2. Compute the function

$$p(t) = \frac{\begin{array}{c}-af'''(t)f(t) - a(\nu+2\delta+a)f''(t)f(t) - a(\delta+a)(\nu+\delta)f'(t)f(t) + af''(t)f'(t)\\ +a(\nu+2\delta+a)f'(t)^2\end{array}}{af(t)[f''(t)+(\nu+2\delta+a)f'(t)+(\delta+a)(\nu+\delta)f(t)]}$$
$$+\frac{\begin{array}{c}a(\delta+a)(\nu+\delta)f'(t)f(t) - \delta af''(t)f(t) - \delta a(\nu+2\delta+a)f'(t)f(t)\\ -\delta a(\delta+a)(\nu+\delta)f^2(t)\end{array}}{af(t)[f''(t)+(\nu+2\delta+a)f'(t)+(\delta+a)(\nu+\delta)f(t)]}.$$

Step 3. Choose $\beta(0)$ and compute the integral $P(t) = \int_0^t p(\tau)\,\mathrm{d}\tau$. Check condition 3:

$$\frac{1}{\beta(0)} + \int_0^{\mathrm{T}} \mathrm{e}^{-P(s)} q(s)\,\mathrm{d}s > 0.$$

Step 4. Compute the function

$$q(t) = \frac{\delta a^2 f^2(t) - af''(t)f^2(t) - a(\nu+2\delta+a)f'(t)f^2(t) - a(\delta+a)(\nu+\delta)f^3(t)}{af(t)[f''(t)+(\nu+2\delta+a)f'(t)+(\delta+a)(\nu+\delta)f(t)]}.$$

Step 5. Apply the formula $\beta(t) = 1/[\mathrm{e}^{P(t)}/\beta(0) + \mathrm{e}^{P(t)}\int_0^t \mathrm{e}^{-P(s)} q(s)\,\mathrm{d}s]$ to compute $\beta(t)$ on the given interval $[0, T]$.

With variable birth rate $\eta(t)$ and constant death rate δ, then the SEIR model becomes

$$S'(t) = \eta(t) - \beta(t)S(t)I(t) - \delta S(t), \tag{31}$$
$$E'(t) = \beta(t)S(t)I(t) - aE(t) - \delta E(t), \tag{32}$$
$$I'(t) = aE(t) - \nu I(t) - \delta I(t), \tag{33}$$
$$R'(t) = \nu I(t) - \delta R(t). \tag{34}$$

In this case, the formula in Step 4 should be

$$q(t) = \frac{\eta(t)a^2 f^2(t) - af''(t)f^2(t) - a(\nu+2\delta+a)f'(t)f^2(t) - a(\delta+a)(\nu+\delta)f^3(t)}{af(t)[f''(t)+(\nu+2\delta+a)f'(t)+(\delta+a)(\nu+\delta)f(t)]}.$$

All other steps in the algorithm remain the same.

Acknowledgements

The UK measles data and birth data were obtained from [17,18]. The authors very much appreciate the efforts of David Earn and Ben Bolker for maintaining these public databases of infectious disease data. The authors thank David Earn for helpful discussion and our sincere thanks to an anonymous referee for identifying the likely source of the three times per year frequency component in our approximation of the transmission rate for measles.

References

[1] R.M. Anderson and R.M. May, *Infectious Diseases of Humans: Dynamics and Control*, Oxford University Press, New York, 1992.
[2] N.G. Becker, *Analysis of Infectious Disease Data*, Chapman and Hall, New York, 1989.
[3] N.G. Becker and T. Britton, *Statistical studies of infectious disease incidence*, J. R. Stat. Soc. Ser. B Stat. Methodol. 61 (1999), pp. 287–307.
[4] O.N. Bjørnstad, B.F. Finkenstädt, and B.T. Grenfell, *Dynamics of measles epidemics: Estimating scaling of transmission rates using a time series SIR model*, Ecol. Monogr. 72 (2002), pp. 169–184.
[5] B.M. Bolker and B.T. Grenfell, *Chaos and biological complexity in measles dynamics*, Proc. R. Soc. Lond. B 251 (1993), pp. 75–81.
[6] M.A. Capistrán, M.A. Moreles, and B. Lara, *Parameter estimation of some epidemic models. The case of recurrent epidemics caused by respiratory syncytial virus*, Bull. Math. Biol. 71 (2009), pp. 1890–1901.
[7] S. Cauchemez and N.M. Ferguson, *Likelihood-based estimation of continuous-time epidemic models from time-series data: Application to measles transmission in London*, J. R. Soc. Interface 5 (2008), pp. 885–897.
[8] J.A. Clarkson and P.E.M. Fine, *The efficiency of measles and pertussis notification in England and Wales*, Int. J. Epidemiol. 14 (1985), pp. 153–168.
[9] S.F. Dowell, *Seasonal variation in host susceptibility and cycles of certain infectious diseases*, Emerg. Infect. Dis. 7 (2001), pp. 369–374.
[10] D.J.D. Earn, P. Rohani, B.M. Bolker, and B.T. Grenfell, *A simple model for complex dynamical transitions in epidemics*, Science 287 (2000), pp. 667–670.
[11] P.E.M. Fine and J.A. Clarkson, *Measles in England and Wales – I: An analysis of factors underlying seasonal patterns*, Int. J. Epidemiol. 11 (1982), pp. 5–14.
[12] R.S. Fujinami, X. Sun, J.M. Howell, J.C. Jenkin, and J.B. Burns, *Modulation of immune system function by measles virus infection: Role of soluble factor and direct infection*, J. Virol. 72 (1998), pp. 9421–9427.
[13] N.C. Grassly and C. Fraser, *Seasonal infectious disease epidemiology*, Proc R. Soc. B Biol. Sci. 273 (2006), pp. 2541–2550.
[14] K. Hadeler, *Parameter identification in epidemic models*, Math. Biosci. 229 (2011), pp. 185–189.
[15] D. He, E.L. Lonides, and A.A. King, *Plug-and-play inference for disease dynamics: Measles in large and small populations as a case study*, J. R. Soc. Interface 7 (2010), pp. 271–283.
[16] H. Hethcote and S.A. Levin, *Periodicity in epidemiological models*, in *Applied Mathematical Ecology*, S.A. Levin, L. Gross, and T.G. Hallam, eds., vol. 18, Springer-Verlag, Berlin, 1989, pp. 193–211.
[17] Infectious disease data. Available at http://people.biology.ufl.edu/bolker/measdata.html.
[18] International Infectious Disease Data Archive. Available at http://iidda.mcmaster.ca/.
[19] R.I. Joh, H. Wang, H. Weiss, and JS. Weitz, *Dynamics of indirectly transmitted infectious diseases with immunological threshold*, Bull. Math. Biol. 71 (2009), pp. 845–862.
[20] M.J. Keeling and R. Rohani, *Modeling Infectious Diseases in Humans and Animals*, Princeton University Press, Princeton, NJ, 2008.
[21] M.J. Keeling, P. Rohani, and B.T. Grenfell, *Seasonally forced disease dynamics explored as switching between attractors*, Phys. D 148 (2001), pp. 317–335.
[22] W.O. Kermack and A.G. McKendrick, *A contribution to the mathematical theory of epidemics*, Proc. R. Soc. Lond. A 115 (1927), pp. 700–721.
[23] D. Kincaid and W. Cheney, *Numerical Analysis: Mathematics of Scientific Computing*, 3rd ed., American Mathematical Society, Brooks Cole, Pacific Grove, CA, 2002.
[24] D. Mollison, *Epidemic Models: Their Structure and Relation to Data*, Cambridge University Press, New York, 1995.
[25] A. Mummert, *Studying the recovery algorithm for the time-dependent transmission rate(s) in epidemic models*, preprint (2011).
[26] A. Mummert, H. Weiss, and H. Wan, *Multiple waves of pandemic influenza*, preprint (2011).
[27] J.A. Patz, T.K. Graczyk, N. Geller, and A.Y. Vittor, *Effects of environmental change on emerging parasitic diseases*, Int. J. Parasitol. 30 (2000), pp. 1395–1405.
[28] J.M. Ponciano and M.A. Capistrán, *First principles modeling of nonlinear incidence rates in seasonal epidemics*, PLoS Comput. Biol. 7 (2011), e1001079. doi:10.1371/journal.pcbi.1001079.
[29] *Sanitary Commissioner for Bengal Reports and Bengal Public Health Reports* (1891–1942), Bengal Secretariat Press, Calcutta and Bengal Government Press, Alipore.
[30] The weekly OPCS (Office of Population Censuses and Surveys) reports, the Registrar General's Quarterly or Annual Reports & various English census reports 1948–1967.
[31] WHO/NREVSS regional reports published in the CDC's Influenza Summary Update (2001).

[32] Wolfram Mathematica Documentation Center.
[33] M. Wolkewitz, M. Dettenkofer, H. Bertz, M. Schumacher, and J. Huebner, *Statistical epidemic modeling with hospital outbreak data*, Stat. Med. 27 (2008), pp. 6522–6531.
[34] Y. Xia, O.N. Bjørnstad, and B.T. Grenfell, *Measles metapopulation dynamics: A gravity model for epidemiological coupling and dynamics*, Am. Nat. 164 (2004), pp. 267–281.
[35] J.A. Yorke and W.P. London, *Recurrent outbreaks of measles, chickenpox and mumps II. Systemtaic differences in contact rates and stochastic effects*, Am. J. Epidemiol. 98 (1973), pp. 469–482.